Transactions of the **13th International Conference on Structural Mechanics in Reactor Technology** (SMiRT 13), Escola de Engenharia - Universidade Federal do Rio Grande do Sul, Porto Alegre, Brazil, August 13-18, 1995

Crack initiation in transportation cask subjected to impact loads. Experimentations and calculations

Yuritzinn, T.[1], Moulin, D.[1], Sert, G.[2]
1) CEA, CEN Saclay , Gif-sur-Yvette Cedex, France
2) Institut de Protection et de Sureté Nucléaire, Fontenay-aux-Roses, France

1 INTRODUCTION

The manufacters of containers for the transport of type B(U) radioactive material must, for the acceptance of these, demonstrate their integrity for the transport of these materials. These must be able to be subjected to the most severe drop conditions required by the IAEA at an ambient temperature of -40°C. This obligation implies that the absence of a risk of a sudden fracture is justified, especially for thick cast iron or forged ferritic steel containers. Recommendations concerning an elastic-plastic treatment of the risks of brittle fracture, i.e., taking plasticity into account in the K_I and J criteria are discussed in TECDOC-717 as could be noted at the Krefeld conference.
To assess the applicability and the validity of the different evaluation methods for the risk of fractures, the IPSN (Institut de Protection et de Sureté Nucléaire) has undertaken, with the support of the CEA/DRN/DMT mechanical engineering laboratories, a research and development program on this subject. Part of this R&D program, with the object of improving our knowledge of the mechanical behavior of a container, has now been completed. The approach adopted was to carry out tests on container mock-ups and cracked rings, then digital simulations of these tests with the Castem-2000 finite-element code for the static case and the Plexus code for the dynamic case. These codes were developed at the CEA, using an elastic-plastic behavior model based on the mechanical characteristics of the material in order to etablish a simplified method for determining J. The objective is to determine the value of J at the time corresponding to crack propagation and compare it with the toughness of the material, the determining mechanical property in this behavior.
The objective of this report is to present the approach adopted for cracked rings, by explaining the choice of this 2D configuration and describing the specific aspects of the method.

2 CHOICE OF CRACKED RING

The first step was to study the mechanical behavior of a container mock-up made of SA 350 LF1 ferritic steel. It consists only of the container body without shock absorbers, cover or components. The well instrumented tests were carried out at the CEA/CESTA and their goals were a drop, with the mock-up cylindrical axis horizontal, from 9 m onto

a rigid target. There were two cases: in the first, the mock-up was without cracks, in the second a longitudinal crack was machined on the open side (the other end being closed) on the internal face of the mock-up. It was noted that the predominant deformation mechanism is the ovalization of the open end of the mock-up, which explains the crack propagation observed at the end of the second test. This leads to the choice of the selected 2D configuration, simple but representative of the bare mock-up: a cracked ring subjected to a vertical ovalization.
The method for determining the value of J corresponding to crack propagation, requires the presence of a flaw resulting in the necessity of machining a longitudinal notch in the rings so as to localize the damage that we want avoid, i.e., crack initiation. To ensure propagation initiation, the longitudinal notch was machined to half the ring thickness.
A characterization run with the material under tension at 3 strain rates ($\dot{\varepsilon} = 0.11$ %s^{-1}, 55 %s^{-1}, 500 %s^{-1}), was carried out at room temperature as well as tests for determining the static and dynamic strengths of the material.

3 STATIC TEST

The static test consisted of a compressive crushing of a cracked ring (A.F. specimen) of the container mock-up. The principle of the test is shown schematically in Figure 2 with the instrumentation. The aim of the test was to induce crack initiation and propagation.
The ring dimensions were Rint = 231 mm, Rext = 321 mm and width = 100 mm. The machined notch is longitudinal, over all the width of the ring and with a depth of 44 mm, fixing it at half the ring thickness. Its is teminated by a 60° angle with a radius of the notch base of less than 0.1 mm.
From the problem symmetry, the mesh used is for a half-width of the cracked ring (Figure 1). To facilitate the modeling, the machined notch geometry was simplified by a line with 15 double nodes. The mesh in the neighborhood of the notch is constructed with concentric circles centered on the crack in order to respect the specifications required for using the G-Theta method in Castem-2000 in determining J.
The mesh includes 7758 nodes of which 90 are double and 5760 elements which consist of 120 6-element nodes and 5640 8-element nodes.
The tensile curve is shown in Figure 4. The main characteristics of the material are given in table 1.
The variation of the force exerted on the ring as a function of the vertical ovalization is shown in Figure 5, for the edge and the center of the ring with the recording of the experimental data. The three-dimensional behavior of the ring is seen by the non-superposition of the curves obtained at the ring center and edge. The agreement between the test and the modeling can be considered acceptable up to around 25 mm, the last value for which the difference between the actual force and the digital value is below 10%.
The extent of the restitution of the energy J is expressed as an integration, over a contour surrounding the singularity, of an expression involving two terms: the strain energy density representing the energy stored in the material taking account of its stress and strain conditions and the stresses on the contour considered. The J integral is invariant with respect to the integration contour.
The variation of the restitution rate of the energy J with the vertical ovalization and the applied force is shown in Figures 6 and 7 for the node at the center of the crack front. The J integrals in the two figures were obtained from elastic and elastic-plastic calculations respectively.

Depending on the case, the relative value of $J_{elastic}$ and $J_{elastoplastic}$ varies. The imposed load or ovalization signifies that in the elastic-plastic computation of J, the load or ovalization is known and consequently the respective ovalization and elastic load are the elastic values calculated with the elastic stiffness. It was seen with the above stress/ovalization curve that for an imposed stress the elastic ovalization is smaller than the real ovalization. Conversely, for a given ovalization, the real stress is smaller than the stress computed elastically.

It can be seen in Figure 8 that for the same compression force, the J integral is greater at the center than at the edge of the ring . This means that the toughness of the material is first reached at the ring center. A crack initiation visible on the side of the ring is thus subsequent to that produced at the ring center.

In the test, the crack initiation was estimated visually for a compression of 57 mm on the edge. Initiation is produced at the ring center for a smaller compression, which would be of the order of 25 mm if it is accepted, for example, that the initiation point is given by Figure 5 at the region where the experimental and computed curves differ by more than 10 %.

It is assumed that the Castem-2000 computation gives the ring behavior for a constant crack length.

The value of J (958 kJ/m^2) corresponding to this compression is higher than the static toughness of the material (891 kJ/m^2), as can be seen in the plot of the variation of J with the vertical ovalization shown in Figure 9 for the ring center.

4 DYNAMIC TESTS

The tests consisted of the dropping of a weight on an A.F specimen of the container mock-up so as to produce crack initiation and propagation. A schematic representation of the dynamic tests is shown in Figure 3 with the experimental arrangement and the instrumentation used by the CEA/CESTA for these tests. The variable parameter in the tests was the height of the drop. The main experimental results are given in table 2.

3D digital simulations of these dynamic tests were made with the Plexus fast dynamics code. The falling weight has an initial velocity of $\sqrt{2gh}$ where h is the drop height. The contact between the ring and the supporting block is made with blocked vertical displacement for the ring points that can be in contact with the supporting block. As carried out here, the modeling is valid only for the first impact of the block on the ring. It cannot simulate the detachment of the ring from the centering component.

The comparison was made for a test where there was little crack propagation.

There is sufficiently good agreement, with a deviation of less than 3 % for the ovalizations at the edge and center obtained, on one hand, by the static elastic-plastic computation for 1040 kN load and, on the other hand, from the dynamic computation at the time that they are at a maximum. The external and internal circumferential deformations for the edge and center from the static (1040 kN load) and dynamic (t = 5 ms) computations are practically identical. It can therefore be accepted that the condition of the stresses and strains in the ring for these two computations is similar. This allows us to consider that the values of the J integral at that time are the same as those of the static computation for the above load.

At the end of the test, a flaw was observed at the bottom of the notch, i.e., an initiation of propagation in the center of the ring. It was assumed that crack initiation was produced at the time when the ovalization of the ring was a maximum. It is 23 mm at the ring center. The value of the extent of the restitution of the energy J then for the dynamic initiation is 868 kJ/m^2. The position of J for dynamic initiation is plotted in Figure 9 and a comparison is made with an evaluation of the dynamic toughness, $J_{0.2}$ dynamic = 888 kJ/m^2. There is a deviation of 2.3%.

6 CONCLUSION

We have presented a method using the J criterion and the Plexus and Castem-2000 finite element codes but it can be seen that the static computation is valid if there is good ovalization. It would be possible to use a simplified method to determine J, e.g., Js (Drubay) in place of Castem-2000.
Our next step is the application of our method to an actual cracked container.

REFERENCES

IAEA Safety Standards No.6, Regulations for the Safe Transport of Radioactive Material 1985 Edition, Vienna 1990
IAEA-TECDOC-717 Guidelines for safe design of shipping packages against brittle fracture, 1993
Krefeld (Germany 1994) "A synthesis of R&D work performed in France about the risk of brittle fracture of transport casks " by D.Moulin, T.Yuritzinn and G.Sert
B.Drubay et al (1993) "Defect assessment procedure : a French approach for fast breeder reactors" ASME PVP vol.266 pp.116-118

table 1:

Young's modulus E (MPa)	215886
$R_{0.002}$ (MPa)	266
Rm (Mpa)	471
$J_{0.2}$ static(kJ/m^2)	891
$J_{0.2}$ dynamic(kJ/m^2)	888
ν	0.3

table 2:

	test 1	test 2	test 3
drop height (m)	9	6	4.5
weight of the block (kg)	510	510	510
maximum shortening of the vertical diameter on impact (mm)	37.	22.	16.4
residual reduction of vertical diameter (mm)	32.	19.6	14.
weight rebound speed (m/s)	3	3.5	3.1
crack length (mm)	8.	4.5	-

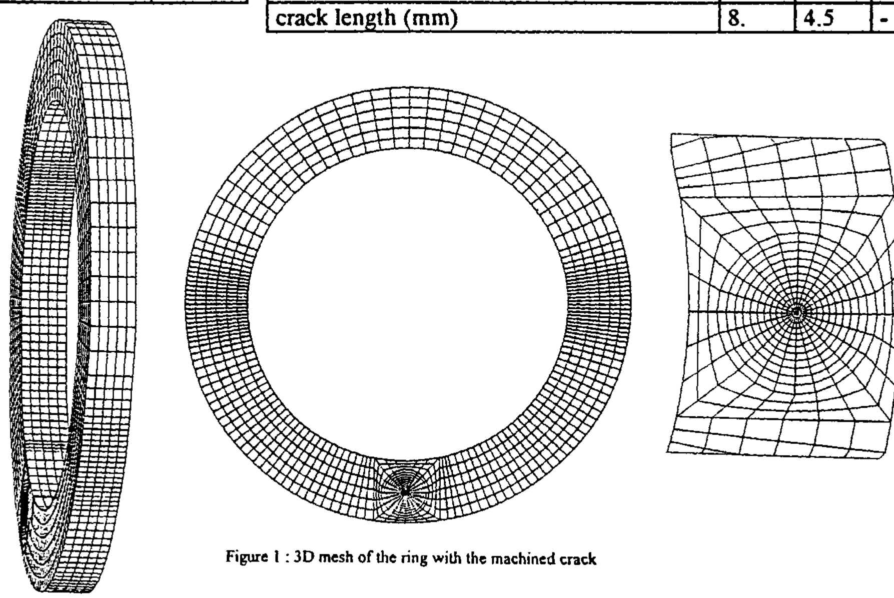

Figure 1 : 3D mesh of the ring with the machined crack

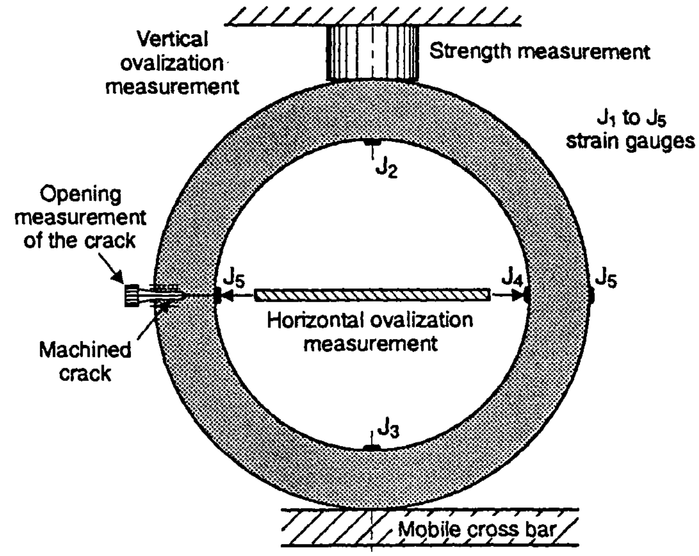

FIGURE 2 - STATIC TEST

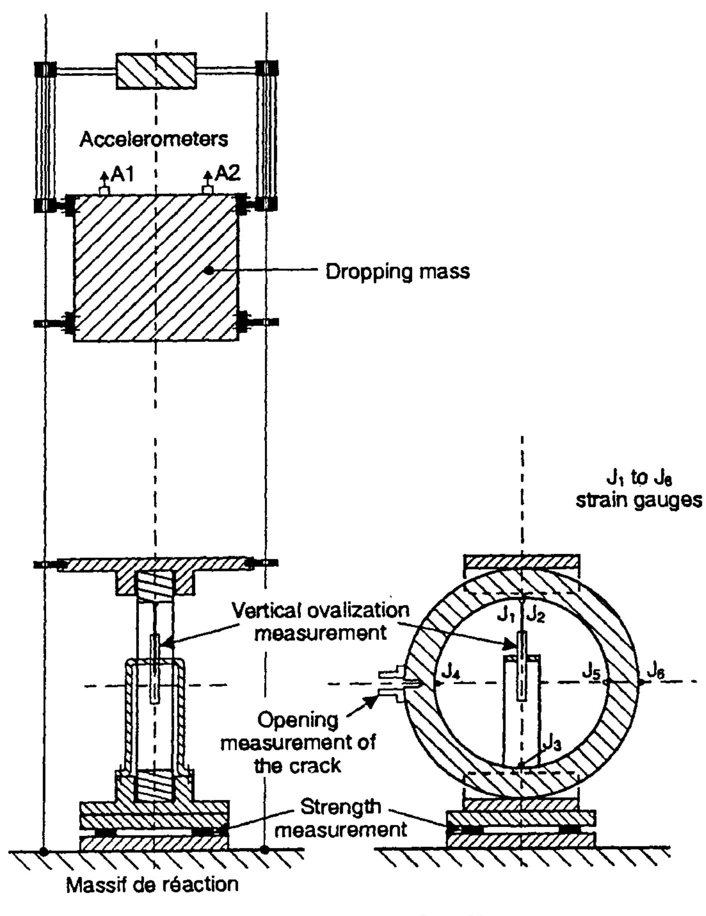

FIGURE 3 - DYNAMIC TEST

figure 4 : Tensile curve at ambient temperature
for SA 350 LF1 steel

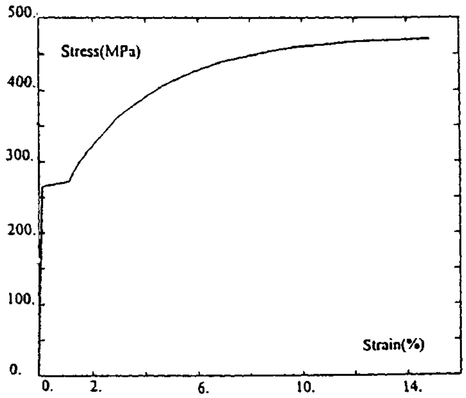

figure 5 : Strength versus ovalization
Static test and Calculation

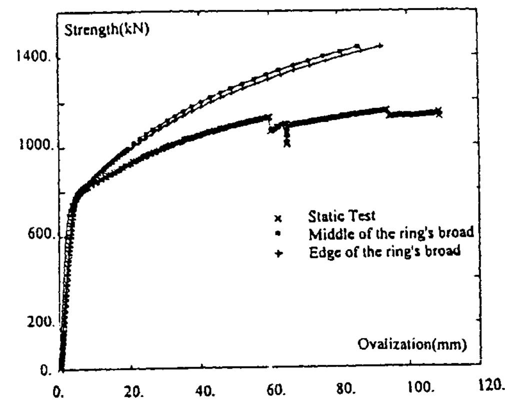

figure 6 : Integral J versus strength
Elastic and plastic calculations

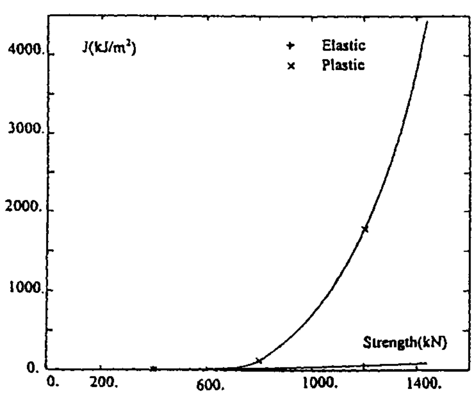

figure 7 : Integral J versus ovalization
Elastic and plastic calculations

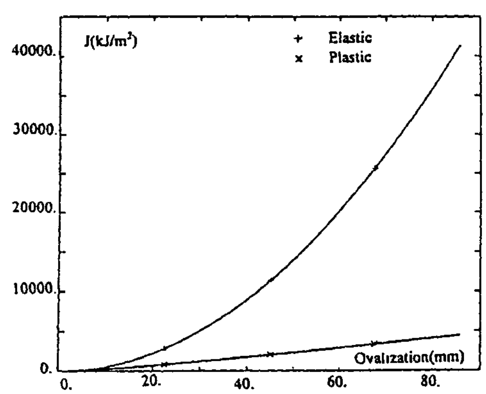

figure 8 : Integral J versus ring's broad
for applied strength

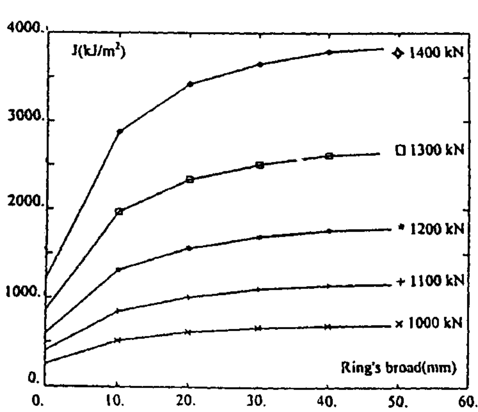

figure 9 : Integral J versus ovalization
Estimation of static and dynamic initiation
of propagation